Journal of Hazardous Materials 472 (2024) 134598

Contents lists available at ScienceDirect

Journal of Hazardous Materials

journal homepage: www.elsevier.com/locate/jhazmat

Exposure to 6-PPD quinone causes damage on mitochondrial complex I/II associated with lifespan reduction in *Caenorhabditis elegans*

Xin Hua [a], Geyu Liang [b], Jie Chao [a], Dayong Wang [a,c,*]

[a] Key Laboratory of Environmental Medicine Engineering of Ministry of Education, Medical School, Southeast University, Nanjing 210009, China
[b] School of Public Health, Southeast University, Nanjing 210009, China
[c] Shenzhen Ruipuxun Academy for Stem Cell & Regenerative Medicine, Shenzhen, China

HIGHLIGHTS

- 6-PPDQ at environmentally relevant concentrations caused mitochondrial dysfunction.
- Complex I/II were involved in induction of 6-PPDQ toxicity on mitochondrial functions.
- Decrease in *gas-1* and *mev-1* expressions mediated 6-PPDQ toxicity on lifespan.
- GAS-1 and MEV-1 regulated 6-PPDQ toxicity by inhibiting insulin peptides and receptor.

GRAPHICAL ABSTRACT

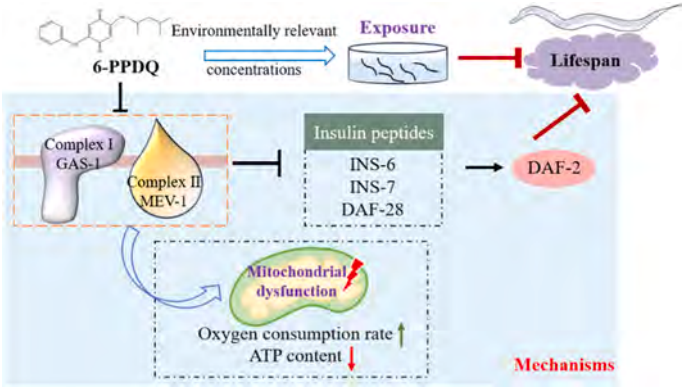

ARTICLE INFO

Keywords:
6-PPDQ
Mitochondrial dysfunction
Mitochondrial complex
Lifespan
Caenorhabditis elegans

ABSTRACT

N-(1,3-dimethylbutyl)-*N*′-phenyl-*p*-phenylenediamine quinone (6-PPDQ) is an emerging pollutant transformed from 6-PPD. However, the effect of 6-PPDQ exposure on mitochondrion and underlying mechanism remains largely unclear. Using *Caenorhabditis elegans* as animal model, exposed to 6-PPDQ at 0.1–10 μg/L was performed form L1 larvae to adult day-1. Exposure to 6-PPDQ (1 and 10 μg/L) could increase oxygen consumption rate and decease adenosine 5′-triphosphate (ATP) content, suggesting induction of mitochondrial dysfunction. Activities of NADH dehydrogenase (complex I) and succinate dehydrogenase (complex II) were inhibited, accompanied by a decrease in expressions of *gas-1*, *nuo-1*, and *mev-1*. RNAi of *gas-1* and *mev-1* enhanced mitochondrial dysfunction and reduced lifespan of 6-PPDQ exposed nematodes. GAS-1 and MEV-1 functioned in parallel to regulate 6-PPDQ toxicity to reduce the lifespan. Insulin peptides and the insulin signaling pathway acted downstream of GAS-1 and MEV-1 to control the 6-PPDQ toxicity on longevity. Moreover, RNAi of *sod-2* and *sod-3*, targeted genes of *daf-16*, caused susceptibility to 6-PPDQ toxicity in reducing lifespan and in causing reactive oxygen species (ROS) production. Therefore, 6-PPDQ at environmentally relevant concentrations (ERCs)

* Corresponding author at: Key Laboratory of Environmental Medicine Engineering of Ministry of Education, Medical School, Southeast University, Nanjing 210009, China.
E-mail address: dayongw@seu.edu.cn (D. Wang).

https://doi.org/10.1016/j.jhazmat.2024.134598
Received 24 March 2024; Received in revised form 25 April 2024; Accepted 10 May 2024
Available online 13 May 2024

potentially caused mitochondrial dysfunction by affecting mitochondrial complexes I and II, which was associated with lifespan reduction by affecting insulin signaling in organisms.

1. Introduction

The antioxidant of *N*-(1,3-dimethylbutyl)-*N*′-phenyl-*p*-phenylenediamine (6-PPD) has been widely used in the production of rubber tires. During aging process of tire particles, 6-PPD can be released into the environment and transforms to 6-PPD quinine (6-PPDQ) [1,2]. Initially, 6-PPDQ was detected frequently in urban tributaries in different countries [3,4]. 6-PPDQ was detected in Australian river with concentrations ranging from 0.4 to 88 ng/L [3]. 6-PPDQ reached up to 1.56 μg/L in urban water system in Pearl River Delta region of China [5]. 6-PPDQ could also be detected in outdoor dusts and sediment with concentrations ranging from 0.043 to 1238 ng/g [6–8]. The 6-PPDQ was bioavailable to organisms, such as mammals [9,10]. After acute exposure, 6-PPDQ induced mortality, abnormal neuronal function, and developmental toxicity in organisms [11–13]. In addition, 6-PPDQ exposure damages several organs in mice, including the liver, lungs, and kidneys [14–16].

Owing to the high sensitivity to environmental exposures [17–19], *Caenorhabditis elegans* has been frequently used to assess toxicity of pollutants at environmentally relevant concentrations (ERCs) [20–23]. Using this animal model, long-term exposure to 6-PPDQ at ERCs (such as 1 and 10 μg/L) could result in intestinal toxicity, neurotoxicity, and reproductive toxicity [24–29]. In addition, both lipid and dopamine metabolisms in *C. elegans* were disrupted by 6-PPDQ exposure at ERCs [30,31]. More recently, it was observed that the lifespan of nematodes could be decreased by exposure to 6-PPDQ [32]. The decrease in lifespan was associated with the activation in several insulin peptides (INS-6, INS-7, and DAF-28) and insulin receptor DAF-2 and the inhibition in FOXO transcriptional factor DAF-16 [32]. Accompanied with these toxicities, obvious 6-PPDQ accumulation was detected in the body of nematodes [32].

Mitochondria play an important role in various cellular process, such as cellular respiration and cell signaling [33]. Meanwhile, mitochondrial dysfunction acts as a key cellular hallmark of toxicity induction of pollutants [34]. Exposure to 6-PPDQ could increase oxygen consumption in zebrafish embryos and rainbow trout gill cells [35,36], suggesting the possible involvement of mitochondria in controlling 6-PPDQ toxicity. However, the association between mitochondrial dysfunction and lifespan reduction in 6-PPDQ exposed nematodes remains unclear. Alteration of mitochondrial complexes could affect longevity and aging-related physiological endpoints in *C. elegans* [37]. In *C. elegans*, mitochondrial function is governed by mitochondrial complexes, such as NADH dehydrogenase (complex I) and succinate dehydrogenase (complex II) [38,39]. The subunits of mitochondrial complex I (GAS-1, NUO-1, and NUO-6) and mitochondrial complex II (MEV-1) are involved in the stress response in *C. elegans* [40].

We assumed that the mitochondrial dysfunction caused by altered mitochondrial complex I/II was associated with reduced lifespan in nematodes. In the current study, we first investigated the effects of 6-PPDQ exposure at ERCs on mitochondrial function and activity of mitochondrial complex I/II. After that, we examined the role of the subunits of mitochondrial complex I/II in controlling mitochondrial activity and lifespan in *C. elegans* after exposure to 6-PPDQ. Moreover, we determined the association between mitochondrial complex I/II subunits and insulin signals during the control of lifespan in 6-PPDQ exposed nematodes. In *C. elegans*, our previous studies have demonstrated the damage of exposure to 6-PPDQ at ERCs on different organs [24–29]. In this study, we further found that exposure to 6-PPDQ at ERCs could further cause damage on nematodes at the organelle level, such as the induction of mitochondrial damage. More importantly, our data highlighted the important role of dysregulated mitochondrial function as the underlying basis for lifespan reduction in 6-PPDQ exposed nematodes. Our results suggested the exposure risk of long-term exposure to 6-PPDQ at ERCs in causing damage on mitochondrial function and complex I/II, which would further led to reduction in lifespan in organisms.

2. Materials and methods

2.1. Animal maintenance and 6-PPDQ exposure

C. elegans was prepared and maintained on normal nematode growth medium (NGM) plates as described previously [41]. During the maintenance, *E. coli* OP50 was fed on NGM plates to satisfy the need of larval development. The used nematode strain was wild-type N2.

6-PPDQ exposure concentrations (0.1, 1, and 10 μg/L) were selected as our previously described [24], which reflects the ERCs [1,5]. Exposure to 6-PPDQ was performed from L1-larvae till to adult day-1 (approximately 4.5 days) [32]. To satisfy the developmental requirements of larval animals, OP50 was added to 6-PPDQ solutions to the final concentration of approximately 5×10^6 colony-forming units [42]. During 6-PPDQ exposure, the working solutions were updated daily. To prepare L1-larvae, the adult hermaphrodites were treating by bleaching solution (0.45 M NaOH and 2% HOCl) to collect eggs [43]. The obtained eggs were allowed to develop on new NGM plates into synchronized L1-larvae.

2.2. Mitochondrial preparation and 6-PPDQ accumulation

Mitochondria were extracted using a mitochondria extraction kit (Jiancheng, Nanjing, China). Approximately 0.1 g nematodes per group were washed with PBS buffer to remove bacteria. After that, ice-precooled nematodes were added to a glass grinder and ground 30 times in an ice bath. The nematode homogenate was transferred to ice-precooled centrifuge tubes and centrifuged at 800 g at 4 ℃ for 5 min, followed by centrifugation at 15000 g at 4 ℃ for 10 min. The mitochondrial precipitate was obtained, washed with 0.2 mL lysate, and resuspended in stock solution for the subsequent experiments.

The accumulation of 6-PPDQ in mitochondria was analyzed by high-performance liquid chromatography with tandem mass spectrometry (HPLC−MS/MS) [32]. The mitochondria were extracted and weighed using the above-mentioned method. Acetonitrile (1 mL) was added to the mitochondrial samples, followed by vigorous crushing for 15 min, which was repeated in triplicates. The combined supernatants were then passed through C18 clean-up tubes and concentrated to near dryness under N_2. Finally, the target was reconstituted in 200 μL acetonitrile for analysis. The concentration of mitochondrial 6-PPDQ was measured using HPLC−MS/MS. Separation was achieved with a BEH-C18 column (2.1 × 100 mm, 1.7 μm). Mitochondrial 6-PPDQ was quantified using external standards with $R^2 > 0.999$. Detailed information regarding the extraction and analysis is provided in Text S1. Three independent experiments were performed. Approximately 1000 nematodes were examined for each group.

The concentration of 6-PPDQ in the exposure solution was then determined. According to analysis, concentrations of 6-PPDQ in 0.1, 1, and 10 μg/L exposure solutions were 0.09 ± 0.06, 1.021 ± 0.38, and 9.125 ± 0.57 μg/L, respectively, which were similar to the nominal concentrations.

2.3. Mitochondrial membrane potential assay

Mitochondrial membrane potential is an important indicator

reflecting mitochondrial viability [44]. Mitochondrial membrane damage was evaluated using a JC-1 probe (Beyotime, China). Under high mitochondrial membrane potential condition, JC-1 can exist in the form of aggregates in the mitochondrial matrix, which will produce red fluorescence [44]. However, JC-1 can exist in the form of monomer producing green fluorescence when mitochondrial membrane potential is low [44]. The nematodes per group were washed with PBS buffer. Nematodes were stained with 1 mL 1 ×JC-1 solution for 2 h at 20 ℃. After the staining, nematodes were transferred to an agarose slide. Red and green fluorescence were detected using a fluorescence microscope. Mitochondrial membrane potential (MMP) was calculated as the ratio of red to green fluorescence. Three independent experiments were performed. Fifty animals were examined for each treatment.

2.4. Oxygen consumption rate (OCR) assay

Alteration of oxygen consumption rate also serve as a useful marker for mitochondrial dysfunction [45]. Using phosphorescent oxygen-sensitive probes, the OCR of mitochondria can be analyzed [45]. After exposure, 100 μL mitochondria per group was added to black fluorescent 96-well plate and incubated with 4 μL BBoxiProbe R01 oxygen fluorescence probe. To avoid the influence of oxygen in the environment, 100 μL oxygen sealer was added to each well. The fluorescence was measured and read at 5 min intervals at an excitation wavelength of 468 nm and emission wavelength of 603 nm. Three independent experiments were conducted. Approximately 1000 nematodes were examined for each group.

2.5. Adenosine 5′-triphosphate (ATP) content assay

ATP plays an important role in various physiological and pathological processes of cells, and the ATP level reflects the state of energy metabolism and mitochondrial function [44]. The ATP content was quantified using an ATP Detection Kit (Beyotime, China) as described [46]. Approximately 0.1 g of nematodes per group were collected. A glass homogenizer was used to lyse the nematodes. The homogenate was centrifuged at 12000 g for 5 min at 4 ℃ to obtain the supernatant. According to manufacturer's instructions, an ATP detection working solution was used to measure the background ATP. The samples or standard liquids were then added and mixed rapidly. The luminescence was measured using a microplate reader (Infinite M200PRO, TECAN). Three independent experiments were conducted. Approximately 1000 nematodes were examined for each group.

2.6. Mitochondrial complex I/ II activities

Activities of mitochondrial complexes are helpfu to evaluate the state of respiratory electron transport chain (ETC) [47]. Enzymatic activity was measured using a Mitochondrial Complex I and II Activity Assay Kit (Sangon, China) [48]. Mitochondria of the nematodes were extracted by adding extraction 1 and grinding 30 times in an ice bath. The supernatant was centrifuged at 11000 g for 15 min at 4 ℃. The supernatant collected to reflect the cytoplasmic fluid was transferred to a new centrifuge tube. The precipitated mitochondria were extracted to obtain mitochondrial fluid. The enzyme activities were measured according to manufacturer's instructions. Complex I was monitored at 340 nm, and complex II was monitored at 600 nm for 60 s using a microplate reader (Infinite M200PRO, TECAN). Three independent experiments were performed. Approximately 1000 nematodes were examined for each group.

2.7. Lifespan assay

The lifespan of nematodes was analyzed as described previously [49]. At the end of exposure, 50 animals from each group were transferred to fresh NGM petri dish. To avoid effect of egg laying, the nematodes were transferred to fresh petri dishes every day. Nematode were repeatedly tapped their head with a platinum wire and no response was considered as death, and the number of surviving nematodes was counted each day. During the lifespan assay, 50% survival was defined as the median lifespan. Significances between lifespan curves were evaluated by Kaplan-Meier software, followed by the Log-rank test. Three independent experiments were conducted.

2.8. Reactive oxygen species (ROS) assay

In *C. elegans*, ROS level reflects the oxidative stress response, which can be estimated using the CM-H_2DCFDA staining method [24]. Nematodes were washed to remove bacteria at the end of exposure. The nematodes were then incubated in solutions containing 1 μM CM-H_2DCFDA for 3 h in darkness. After washing three times using K buffer, the animals were transferred onto 2% agarose pad. Intestinal fluorescent signals in nematodes were detected using laser confocal microscope under the FITC signaling pathway (excitation/emission wavelengths: 488/510 nm). After normalization to intestinal autofluorescence, intensity of intestinal ROS signals was semi-quantified using Image J software. Fifty animals were analyzed for each exposure.

2.9. Genes expression analysis

Gene expression was analyzed by quantitative real-time polymerase chain reaction (qRT-PCR). Nematodes were allowed to settle naturally and the supernatant was removed at the end of exposure. TRIzol was used to extract RNA, and the quality was assessed based on the value of A260/A280 using a Nanodrop One. Three micrograms of mRNA from each sample were added to synthesize cDNA. qRT-PCR was conducted using SYBR qRT-PCR mix (Vazyme, China). Relative expression levels of examined genes were calculated using the 2^-ΔΔCt method. The analyzed genes were normalized to the reference gene *tba-1* [50]. Three replicates were carried out. The primers are shown in Table S1.

2.10. RNA interference (RNAi)

To prepare RNAi clones, gene constructs for RNAi were generated in L4440 (an empty vector), and confirmed by sequencing. The constructs were subsequently transformed into *E. coli.* HT115 [51]. Before the experiment, RNAi cells were cultured on NGM plates containing 1 mM isopropylthiogalactoside for 24 h to induce double-stranded RNA expression. Nematodes were fed RNAi and the progeny were used for the exposure experiment. The control consisted of HT115 expressing L4440 [52]. qRT-PCR was used to assess RNAi efficiency (Fig. S1).

2.11. Data analysis

Data are expressed as mean ± standard deviation (SD). Statistical analysis was performed using SPSS Statistics 25.0 software. The statistical significance between different groups was analyzed using one-way or two-way analysis of variance (ANOVA) followed by Dunnett's test. Two-way ANOVA was performed to compare the significance among different treatment groups. Statistical significance was set at a probability level of 0.01.

3. Results

3.1. Mitochondrial accumulation of 6-PPDQ in C. elegans

Firstly, 6-PPDQ accumulation in the mitochondria of *C. elegans* was assessed after exposure to 6-PPDQ. No accumulation of 6-PPDQ in the mitochondria was observed in nematodes exposed to 6-PPDQ at 0.1 μg/L (Fig. 1A). In contrast to this, after exposure to 1 and 10 μg/L 6-PPDQ, the internal concentration of 6-PPDQ reached 0.021 ng/mg and 0.888 ng/mg mitochondria weight, respectively (Fig. 1A). Meanwhile,

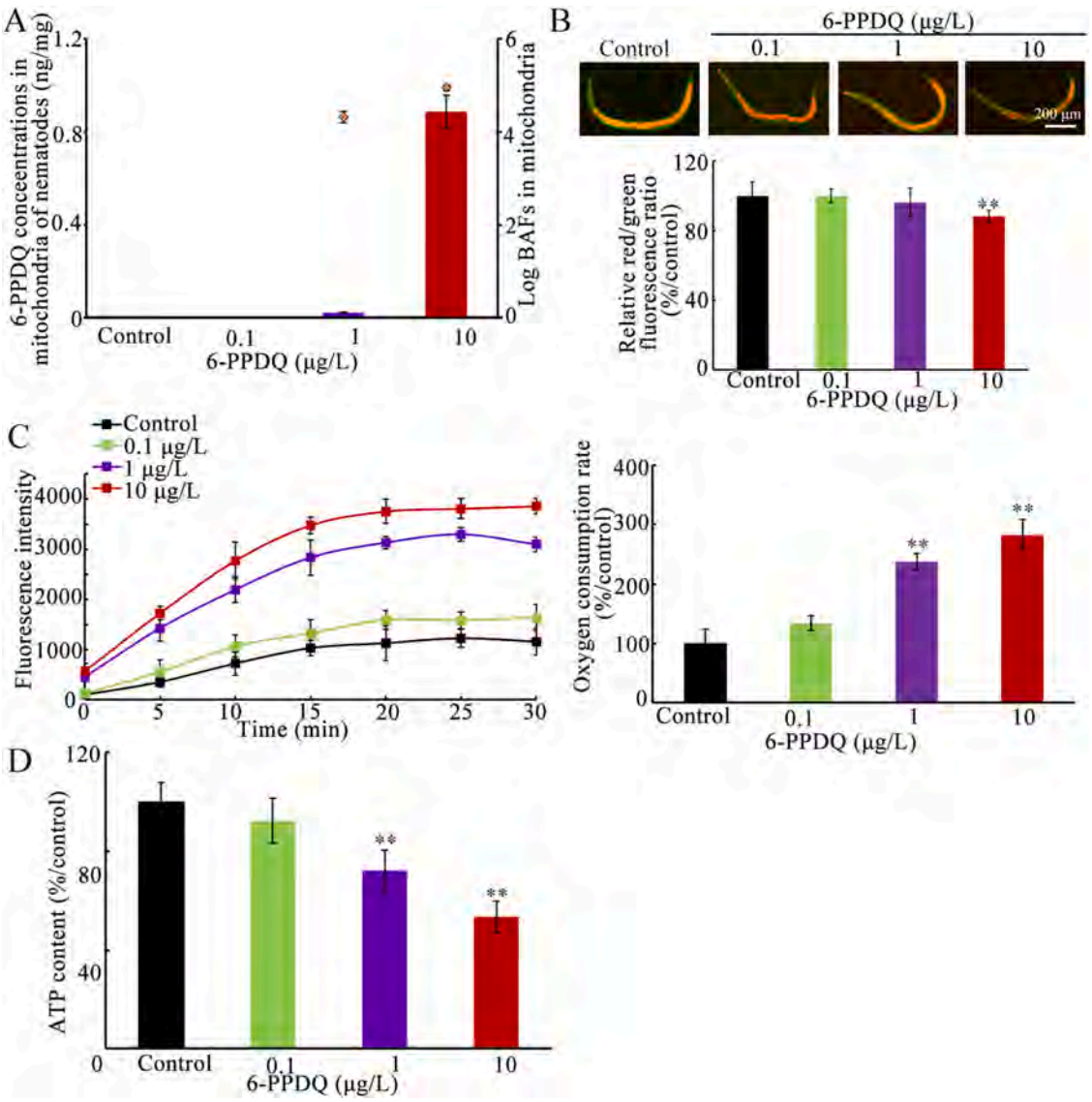

Fig. 1. Mitochondrial 6-PPDQ accumulation and effects of 6-PPDQ exposure on mitochondrial membrane potential and functions. (A) Internal 6-PPDQ concentrations and log BAFs in mitochondrion of nematodes exposed to 6-PPDQ at 0.1, 1 and 10 μg/L. The column represents the concentrations of 6-PPDQ in mitochondria, and the scatter represents log BAF value. BAFs = $C_{mit}/C_{6\text{-PPDQ}}$, where C_{mit} is the concentration of 6-PPDQ in mitochondria of *C. elegans* and $C_{6\text{-PPDQ}}$ is the concentration of 6-PPDQ in working solution. (B) Mitochondrial membrane potential of nematodes after 6-PPDQ exposure. (C) Oxygen consumption curve of mitochondria and comparison of oxygen consumption rate at 30 min after 6-PPDQ exposure. (D) ATP content of nematodes after 6-PPDQ exposure. Bars represent means ± SD. $^{**}P < 0.01$ vs control.

bioaccumulation factor (BAFs) analysis showed that log BAF values of 6-PPDQ ranged from 4.32 to 4.95, which further indicated the bioaccumulation of 6-PPDQ in mitochondria of *C. elegans* (Fig. 1A).

3.2. 6-PPDQ exposure affected mitochondrial membrane potential and mitochondrial function

To examine whether 6-PPDQ exposure affected MMP, the JC-1 red/green fluorescence ratio was evaluated. In 0.1 and 1 μg/L 6-PPDQ exposed nematodes, the MMP was comparable to that of the control (Fig. 1B). Conversely, a moderate but significant fall in MMP was observed in 6-PPDQ (10 μg/L) exposed nematodes (Fig. 1B).

OCR and ATP content were used as parameters to assess mitochondrial function. After 6-PPDQ exposure, the oxygen consumption rapidly increased and reached a plateau at 20 min (Fig. 1C). In terms of both oxygen consumption and ATP content, there was no significant increase in nematodes exposed to 6-PPDQ at 0.1 μg/L in comparison to the control group (Figs. 1C and 1D). By contrast, the OCR was significantly increased in nematodes exposed to 6-PPDQ at 1 and 10 μg/L (Fig. 1C). Moreover, exposure to 6-PPDQ (1 and 10 μg/L) significantly decreased ATP content compared to that of the control (Fig. 1D). Therefore, 6-PPDQ exposure could affect mitochondrial function.

3.3. 6-PPDQ exposure reduced activities of mitochondrial complexes I and II

Considering the contribution of mitochondrial complexes I and II to mitochondrial functions, complex I and complex II enzyme activities were examined in nematodes exposed to 6-PPDQ. Exposure to 6-PPDQ at 0.1 μg/L did not cause alteration in activities of complexes I and II (Fig. 2A). Similarly, the transcription levels of *gas-1*, *nuo-1*, *nuo-6*, and *mev-1* genes encoding components on mitochondrial complexes I and II were not altered in nematodes exposed to 6-PPDQ at 0.1 μg/L (Fig. 2B). Conversely, exposure to 6-PPDQ (1 and 10 μg/L) induced the decreased activities of complexes I and II in nematodes (Fig. 2A). In addition, after exposure to 6-PPDQ (1 and 10 μg/L), the expressions of *gas-1*, *nuo-1*, and

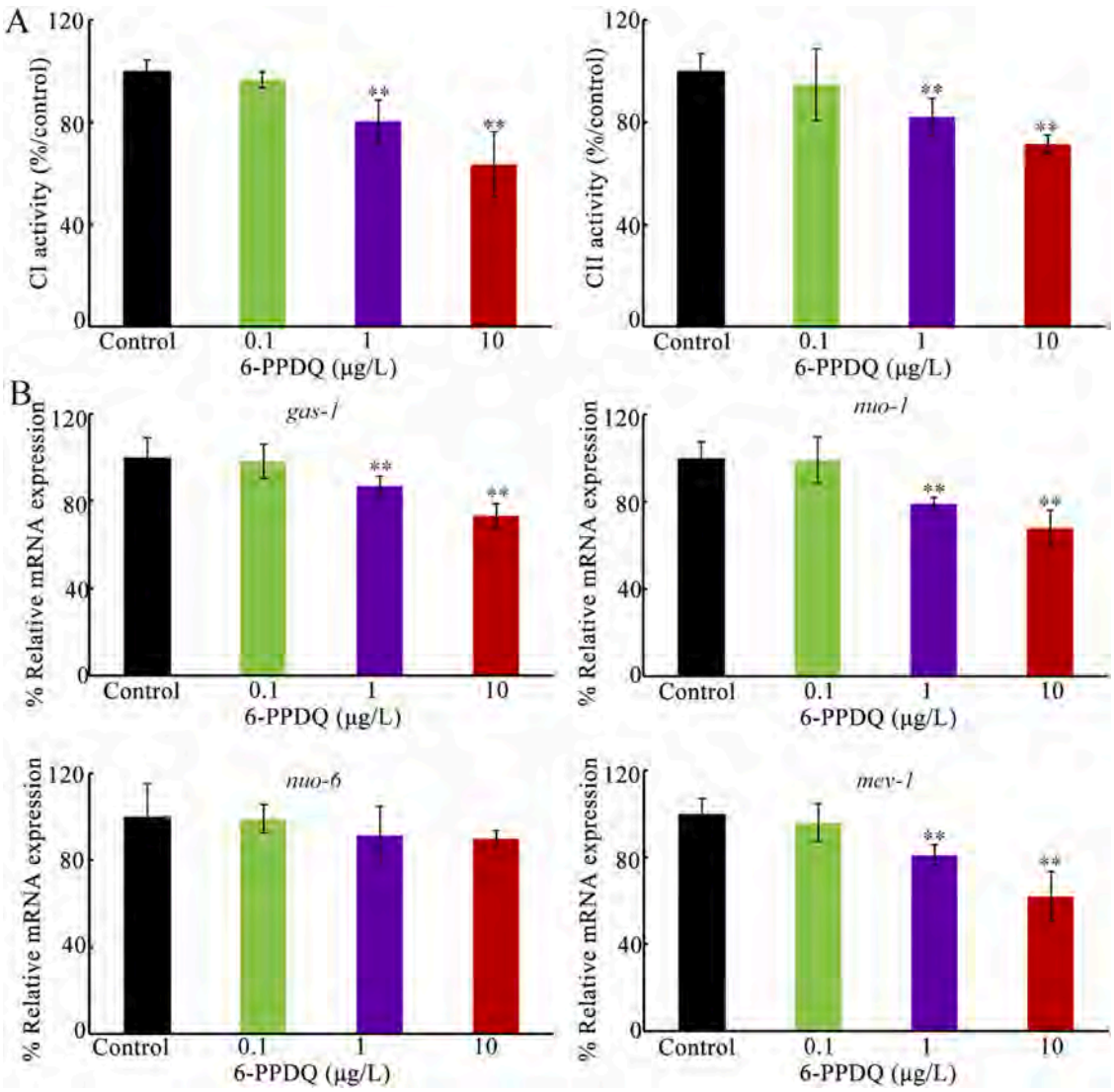

Fig. 2. Effects of 6-PPDQ exposure on activities of mitochondrial complex I and II (A) and expressions of genes (*gas-1*, *nuo-1*, *nuo-6*, and *mev-1*) encoding components in mitochondrial complex I and II (B). Bars represent means ± SD. $^{**}P < 0.01$ vs control.

mev-1 were decreased (Fig. 2B). Nevertheless, the expression of *nuo-6* was not changed by 6-PPDQ exposure (Fig. 2B).

3.4. RNAi of gas-1, nuo-1 and mev-1 affected mitochondrial functions in 6-PPDQ exposed nematodes

Among genes encoding components on mitochondrial complexes I and II, considering that only *gas-1*, *nuo-1*, and *mev-1* expressions were altered by 6-PPDQ exposure, RNAi of *gas-1*, *nuo-1*, and *mev-1* was further carried out. The 10 μg/L for 6-PPDQ was selected in RNAi experiments due to significant mitochondrial dysfunction and decrease in mitochondrial complexes activities observed in nematodes under this concentration exposure. Following 6-PPDQ exposure, the relative OCR (6-PPDQ/control) in *gas-1(RNAi)*, *nuo-1(RNAi)*, and *mev-1(RNAi)* nematodes was higher than that in the wild-type (L4440) (Fig. 3A). Meanwhile, following being subjected to 6-PPDQ, the relative ATP content (6-PPDQ/control) in *gas-1(RNAi)*, *nuo-1(RNAi)*, and *mev-1(RNAi)* nematodes was lower in comparison to that in the wild-type (L4440) (Fig. 3B). Thus, the RNAi of *gas-1*, *nuo-1*, and *mev-1* enhanced oxygen consumption and inhibited ATP content after 6-PPDQ exposure.

3.5. GAS-1 and MEV-1 regulated longevity in 6-PPDQ exposed nematodes by affecting insulin signaling pathway

In *C. elegans*, alteration in mitochondrial complexes are associated with lifespan regulation [53]. RNAi of *gas-1* and *mev-1* significantly decreased the relative lifespan (6-PPDQ/control) of nematodes subjected to 6-PPDQ treatment compared to that in the wild-type (L4440) (Figs. 4A and 4C). However, the relative lifespan (6-PPDQ/control) of *nuo-1(RNAi)* nematodes was comparable to that of the control nematodes (Fig. 4B). Therefore, 6-PPDQ toxicity on the lifespan of nematodes was mediated by changes in GAS-1 and MEV-1 expressions.

We further investigated the interaction between GAS-1 and MEV-1 in controlling 6-PPDQ toxicity on lifespan. After the 6-PPDQ exposure, lifespans of *mev-1(RNAi);gas-1(RNAi)* nematodes were significantly shorter than those of *gas-1(RNAi)* and *mev-1(RNAi)* nematodes (Fig. 4D). Therefore, GAS-1 and MEV-1 acted in parallel to control 6-PPDQ toxicity on longevity.

Insulin peptides (INS-6, INS-7, and DAF-28) played a key role in controlling 6-PPDQ toxicity on longevity [32]. In 6-PPDQ exposed nematodes, RNAi of *gas-1* significantly increased the transcription levels of *ins-6*, *ins-7*, and *daf-28* (Fig. 5A). In addition, the transcriptional levels of these three genes were dramatically upregulated by RNAi of *mev-1* in

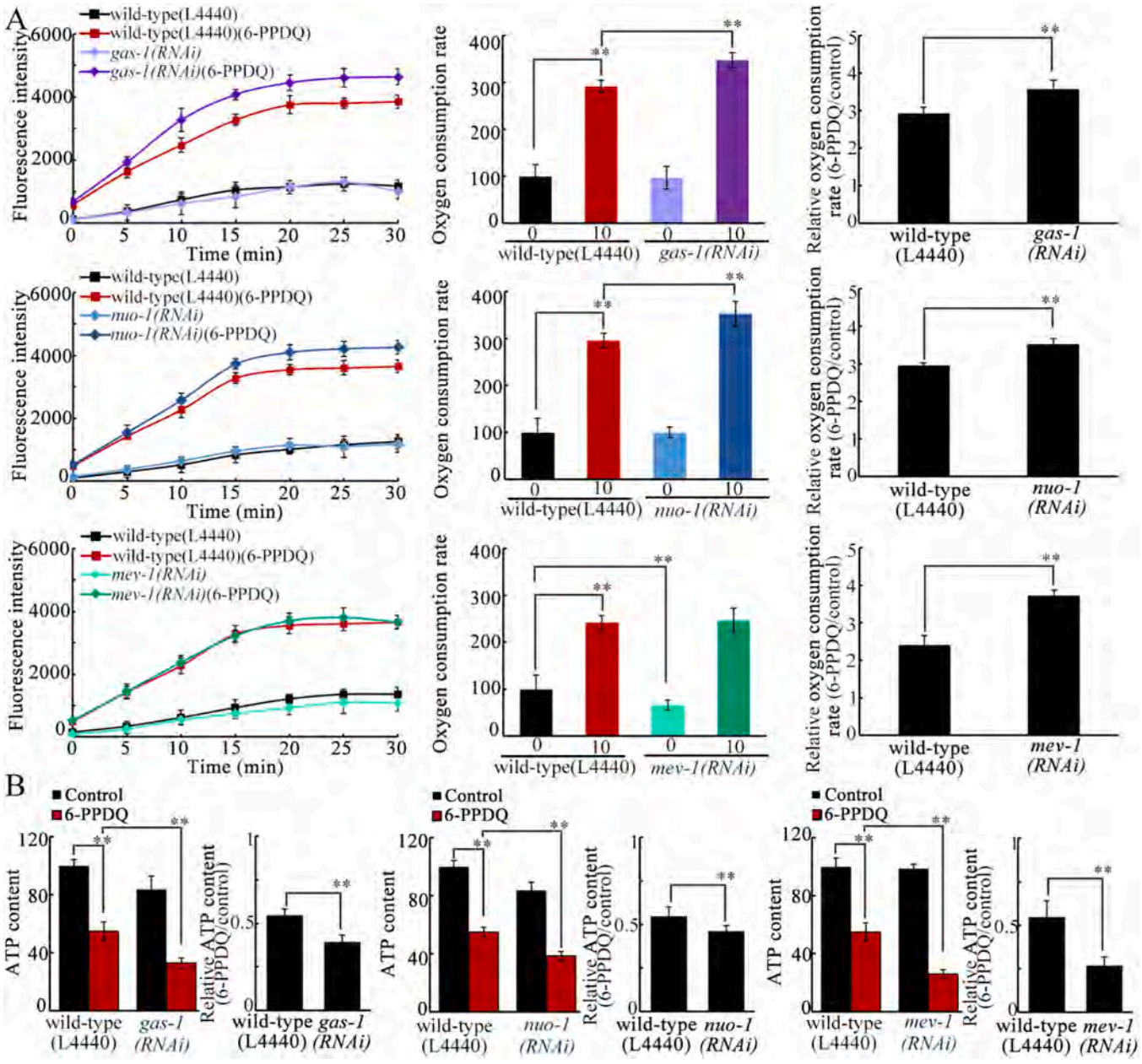

Fig. 3. Effect of RNAi of *gas-1*, *nuo-1*, and *mev-1* on oxygen consumption (A) and ATP content (B) in 6-PPDQ exposed nematodes. Exposure concentration of 6-PPDQ was 10 μg/L. Control, without 6-PPDQ exposure. L4440, empty vector. Bars represent means ± SD. $^{**}P < 0.01$.

C. elegans subjected to 6-PPDQ (Fig. 5B). Therefore, insulin peptide genes could be altered by RNAi of *gas-1* and *mev-1* in nematodes exposed to 6-PPDQ.

Following 6-PPDQ exposure, the RNAi of *ins-6*, *ins-7*, and *daf-28* suppressed the susceptibility of *gas-1(RNAi)* nematodes to 6-PPDQ toxicity in reducing lifespan (Fig. 5C). Similarly, the lifespan of *mev-1 (RNAi)* nematodes was prolonged when RNAi of these three genes was performed in *C. elegans* subjected to 6-PPDQ treatment (Fig. 5D). Thus, our findings suggest that GAS-1 and MEV-1 acted upstream of these three insulin peptides to control 6-PPDQ toxicity on lifespan.

To further determine whether GAS-1 and MEV-1 regulated 6-PPDQ toxicity on lifespan by affecting the insulin signaling pathway, the expressions of genes in insulin signaling pathway in 6-PPDQ exposed *gas-1 (RNAi)* and *mev-1(RNAi)* nematodes were examined. Following being subjected to 6-PPDQ exposure, the transcript levels of *daf-2*, *age-1*, *akt-1*, and *akt-2* were increased, and the transcript level of *daf-16* was decreased by RNAi of *gas-1* and *mev-1* (Figs. 6A and 6B).

The genetic interaction between DAF-2 and GAS-1 or MEV-1 in controlling the effect of 6-PPDQ toxicity on lifespan was further examined. After 6-PPDQ exposure, the lifespans of *daf-2(RNAi);gas-1(RNAi)* and *daf-2(RNAi);mev-1(RNAi)* nematodes were comparable to those of *daf-2(RNAi)* nematodes (Figs. 6C and 6D). RNAi of *daf-2* significantly suppressed the reduced lifespan of *gas-1(RNAi)* and *mev-1(RNAi)* nematodes after exposure to 6-PPDQ (Figs. 6C and 6D). Therefore, GAS-1 and MEV-1 acted upstream of DAF-2 to regulate 6-PPDQ toxicity in reducing lifespan.

3.6. RNAi of gas-1 and mev-1 decreased expression of genes encoding mitochondrial Mn-SODs in 6-PPDQ exposed nematodes

In *C. elegans*, manganese superoxide dismutases (Mn-SODs), including SOD-2 and SOD-3, are involved in the protection from mitochondrial ROS damage [54]. Our previous study demonstrated a decrease in *sod-3* expression in *daf-16(RNAi)* nematodes exposed to

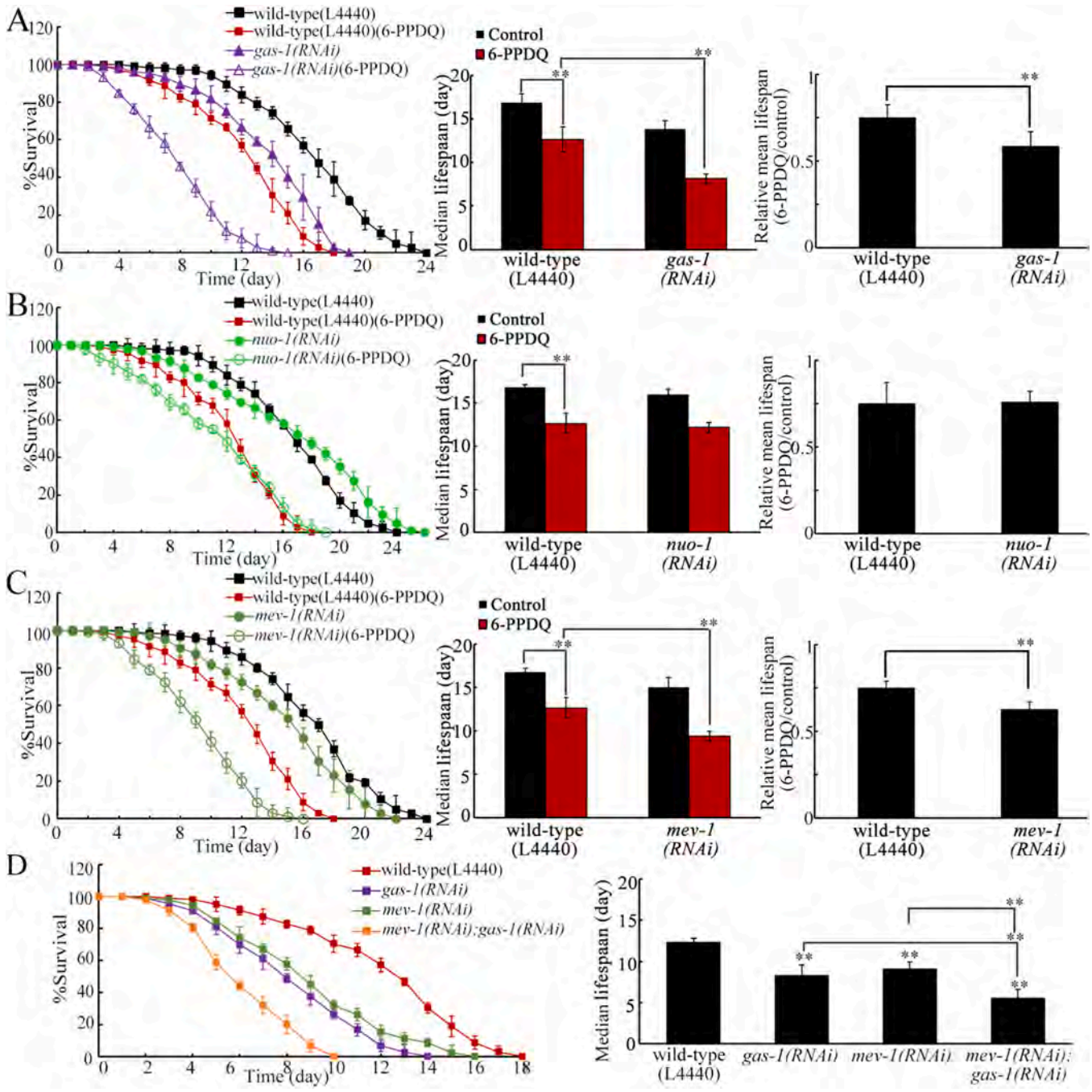

Fig. 4. Effect of RNAi of *gas-1*, *nuo-1*, and *mev-1* on lifespan in 6-PPDQ exposed nematodes. (A) Effect of RNAi of *gas-1* on lifespan in 6-PPDQ exposed nematodes. (B) Effect of RNAi of *nuo-1* on lifespan in 6-PPDQ exposed nematodes. (C) Effect of RNAi of *mev-1* on lifespan in 6-PPDQ exposed nematodes. (D) Genetic interaction between *gas-1* and *mev-1* in regulating lifespan in 6-PPDQ exposed nematodes. Exposure concentration of 6-PPDQ was 10 μg/L. Control, without 6-PPDQ exposure. L4440, empty vector. Bars represent means ± SD. $^{**}P < 0.01$.

6-PPDQ [32]. The expression of *sod-2* was also suppressed in *daf-16 (RNAi)* nematodes exposed to 6-PPDQ (Fig. S2), suggesting the potential role of SOD-2 and SOD-3 as downstream of DAF-16 during the regulation of 6-PPDQ toxicity. We also observed that, after 6-PPDQ exposure, the relative expressions of *sod-2* (6-PPDQ/control) and *sod-3* (6-PPDQ/control) were significantly reduced by RNAi of *gas-1* or *mev-1* (Figs. 7A and 7B).

The relative median lifespans of *sod-2(RNAi)* (6-PPDQ/control) and *sod-3(RNAi)* (6-PPDQ/control) nematodes were lower than those of wild-type (L4440) nematodes (Fig. 7B), suggesting the susceptibility of *sod-2(RNAi)* and *sod-3(RNAi)* nematodes to 6-PPDQ toxicity in reducing lifespan. Following 6-PPDQ exposure, RNAi of *sod-2* and *sod-3* further caused severe stimulation of ROS generation compared to that in the wild-type(L4440) (Fig. 7C).

4. Discussion

6-PPDQ was identified as an emerging pollutant with high toxicity for aquatic animals [1]. Previous studies implied that 6-PPDQ toxicity was associated with mitochondrial damage [25,26,55]. However, the association between mitochondrial dysfunction and 6-PPDQ toxicity on longevity in organism remains unclear. In this study, we focused on the examination of mitochondrial function and activities of mitochondrial complex I/II following long-term exposure to 6-PPDQ at ERCs. In

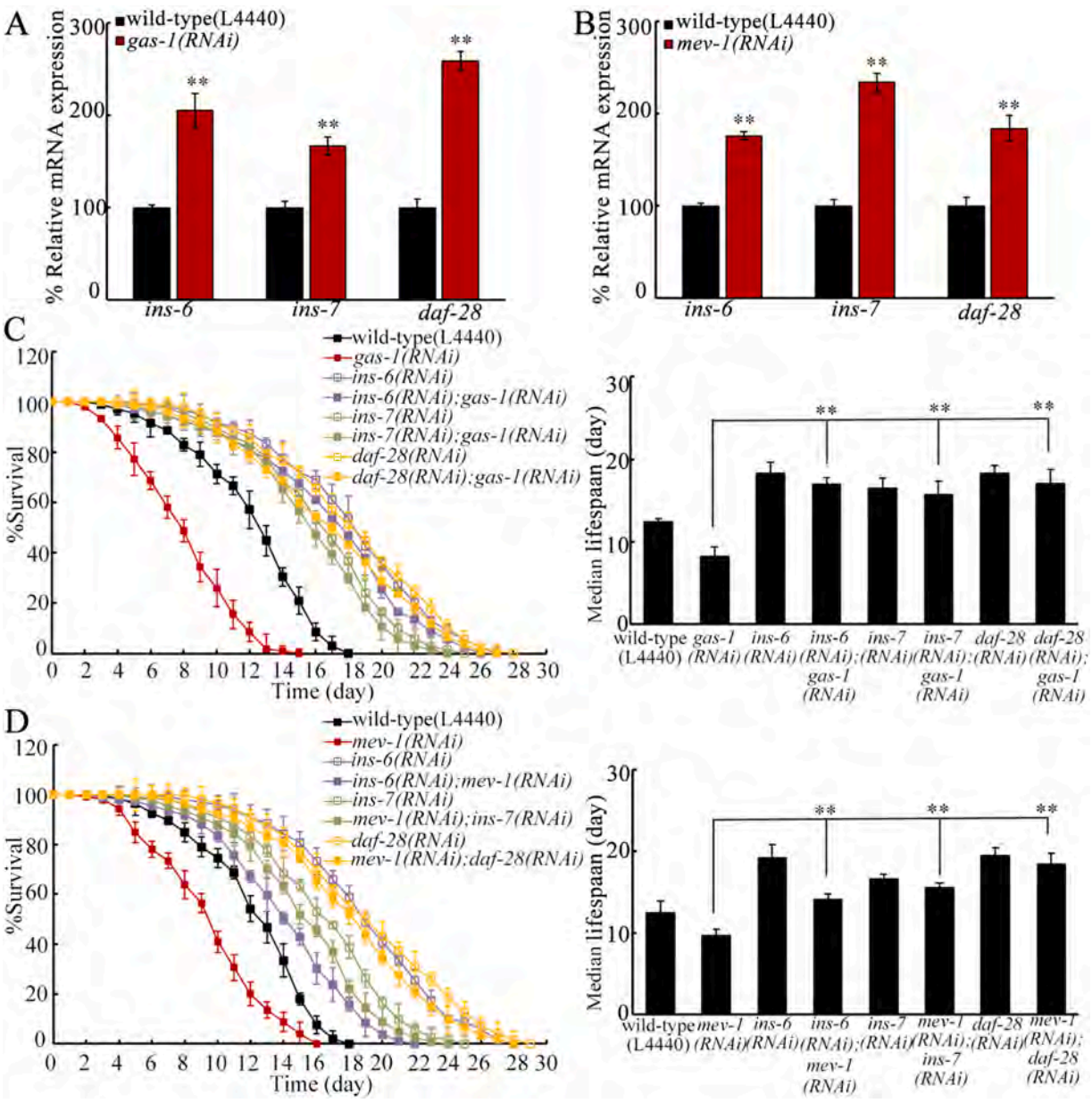

Fig. 5. Genetic interaction between insulin peptides and GAS-1 or MEV-1 in regulating 6-PPDQ toxicity in reducing lifespan. (A) Effect of RNAi of *gas-1* on expressions of *ins-6*, *ins-7*, and *daf-28* in 6-PPDQ-exposed nematodes. Bars represent means ± SD. $^{**}P < 0.01$ vs wild-type(L4440). (B) Effect of RNAi of *mev-1* on expressions of *ins-6*, *ins-7*, and *daf-28* in 6-PPDQ-exposed nematodes. Bars represent means ± SD. $^{**}P < 0.01$ vs wild-type(L4440). (C) Genetic interaction between GAS-1 and INS-6, INS-7, or DAF-28 in controlling 6-PPDQ toxicity on lifespan. Bars represent means ± SD. $^{**}P < 0.01$. (D) Genetic interaction between MEV-1 and INS-6, INS-7, or DAF-28 in controlling 6-PPDQ toxicity on lifespan. Exposure concentration of 6-PPDQ was 10 μg/L. L4440, empty vector. Bars represent means ± SD. $^{**}P < 0.01$.

addition, the relationship between mitochondrial complex I/II subunits and insulin signaling pathway during the control of lifespan of 6-PPDQ exposed nematodes was further determined.

4.1. 6-PPDQ at ERCs caused mitochondrial damage

6-PPDQ was identified as an emerging pollutant with high toxicity for aquatic animals [1]. Current studies have shown 6-PPDQ toxicity with respect to various aspects [4,56,57]. The bioavailability of 6-PPDQ to organisms has also been observed [10]. Our previous study has demonstrated the accumulation of 6-PPDQ in *C. elegans* [32]. 6-PPDQ has also been detected in several organs in mice, including liver, kidneys, and lungs [9,14]. We detected remarkable accumulation of 6-PPDQ in the mitochondria of *C. elegans* subjected to 6-PPDQ at 1 and 10 μg/L (Fig. 1A). This observation suggests that exposure to 6-PPDQ potentially targets the mitochondria and causes mitochondrial damage.

Previous studies have indicated that 6-PPDQ exposure increased the OCR in zebrafish and rainbow trout cells [35,36], which implies the induction of mitochondrial dysfunction. According to our observations, the OCR was considerably increased in nematodes exposed to 6-PPDQ at 1 and 10 μg/L (Fig. 1C). Consistently, 6-PPDQ at 20 μg/L increased the OCR by 100% compared to that in the control in fish cells [36]. Additionally, the ATP content was considerably reduced after exposure to 6-PPDQ at 1 and 10 μg/L (Fig. 1D). In the environment, 6-PPDQ can be found at doses varying from ng/L to μg/L [58,59]. In Seattle, 6-PPDQ was identified to have a peak concentration of 19 μg/L [1]. These findings suggest that 6-PPDQ at ERCs could cause the mitochondrial dysfunction. In addition, our data further suggested that the damage to

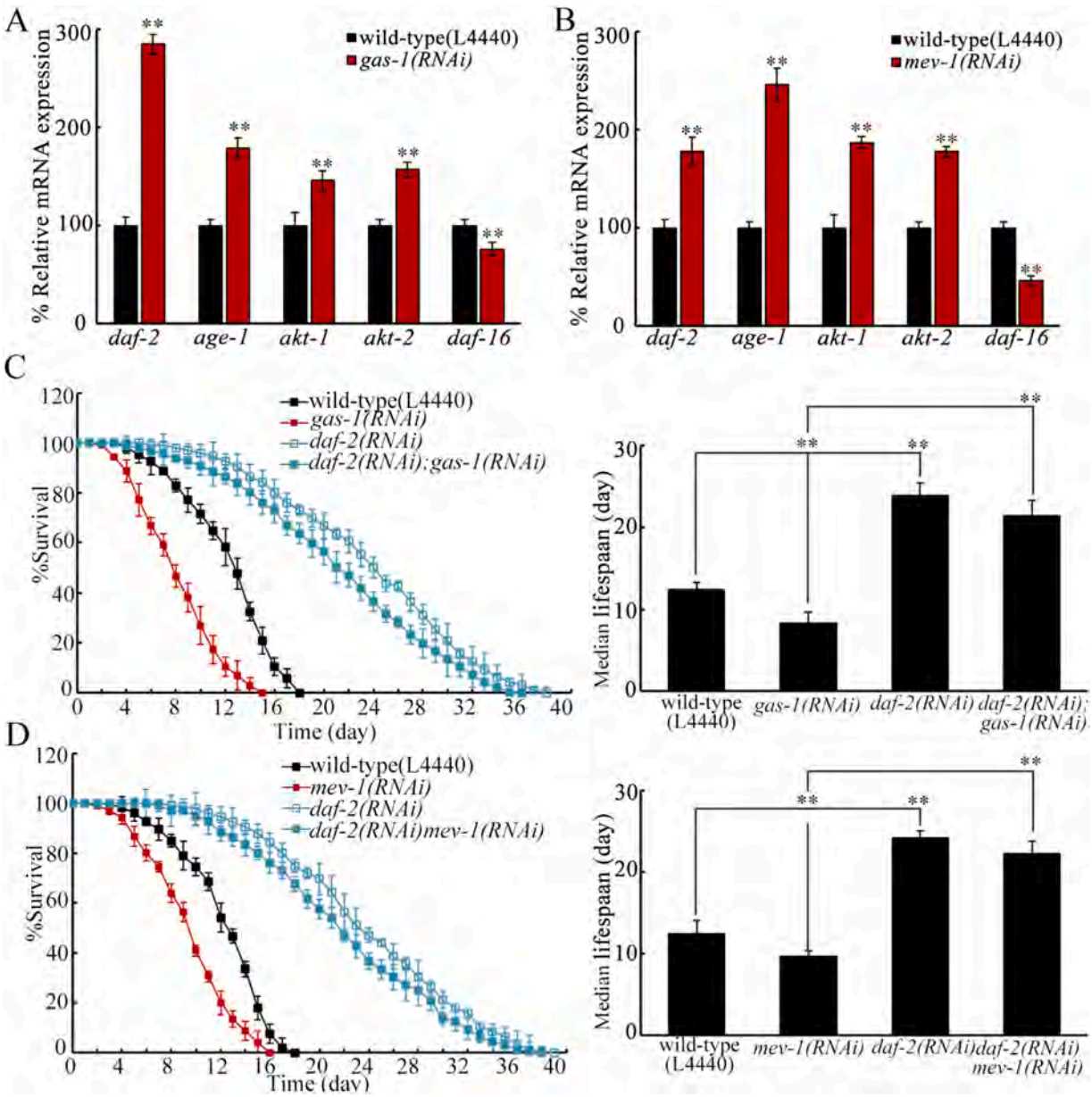

Fig. 6. Genetic interaction between insulin receptor DAD-2 and GAS-1 or MEV-1 in regulating 6-PPDQ toxicity in reducing lifespan. (A) Effect of RNAi of *gas-1* on expressions of *daf-2*, *age-1*, *akt-1*, *akt-2*, and *daf-16* in 6-PPDQ exposed nematodes. Bars represent means ± SD. $^{**}P < 0.01$ vs wild-type(L4440). (B) Effect of RNAi of *mev-1* on expressions of *daf-2*, *age-1*, *akt-1*, *akt-2*, and *daf-16* in 6-PPDQ exposed nematodes. Bars represent means ± SD. $^{**}P < 0.01$ vs wild-type(L4440). (C) Genetic interaction between DAF-2 and GAS-1 to control 6-PPDQ toxicity on lifespan. Bars represent means ± SD. $^{**}P < 0.01$. (D) Genetic interaction between DAF-2 and MEV-1 to control 6-PPDQ toxicity on lifespan. Exposure concentration of 6-PPDQ was 10 μg/L. L4440, empty vector. Bars represent means ± SD. $^{**}P < 0.01$.

mitochondrial function was attributed to the accumulation of 6-PPDQ in the mitochondria of the nematodes. Mitochondrial membrane potential is an important marker for healthy mitochondria [60]. Nevertheless, only 10 μg/L 6-PPDQ could decrease the MMP (Fig. 1B). Therefore, exposure to 6-PPDQ at ERCs may mainly damage mitochondrial function but not mitochondrial membrane permeability.

4.2. Exposure to 6-PPDQ disrupted mitochondrial complexes I and II

Mitochondrial respiratory chain complexes play key roles in electron transport chain and then modulate mitochondrial functions [61]. Complex I (NADH dehydrogenase) and Complex II (succinate dehydrogenase) are the important components of mitochondrial complexes and the gatekeepers for initiating the electron transport chain [62]. In *C. elegans*, GAS-1, NUO-1, and NUO-6 are mitochondrial complex I subunits, and MEV-1 is a component on mitochondrial complex II [40]. In nematodes, exposure to 6-PPDQ at 1 and 10 μg/L decreased the activity of complex I, accompanied by the decreased expression of *gas-1* and *nuo-1* (Fig. 2). Meanwhile, the decreased activity of complex II together with the decreased *mev-1* expression were observed in *C. elegans* exposed to 1 and 10 μg/L (Fig. 2). Our findings offer a crucial biochemical foundation for the toxic effects of 6-PPDQ exposure on mitochondrial function. Moreover, RNAi of *gas-1*, *nuo-1* and *mev-1* strengthened 6-PPDQ toxicity on mitochondrial functions, as reflected by the alteration in the endpoints of the oxygen consumption rate and ATP content (Fig. 3). On one hand, this conformed previous conjecture that 6-PPDQ may affect the mitochondrial respiratory chain [36]. On the other hand, this further supported the association of alteration in complexes I and II with induction of mitochondrial dysfunctions in nematodes exposed to 6-PPDQ. Therefore, exposure to 6-PPDQ potentially

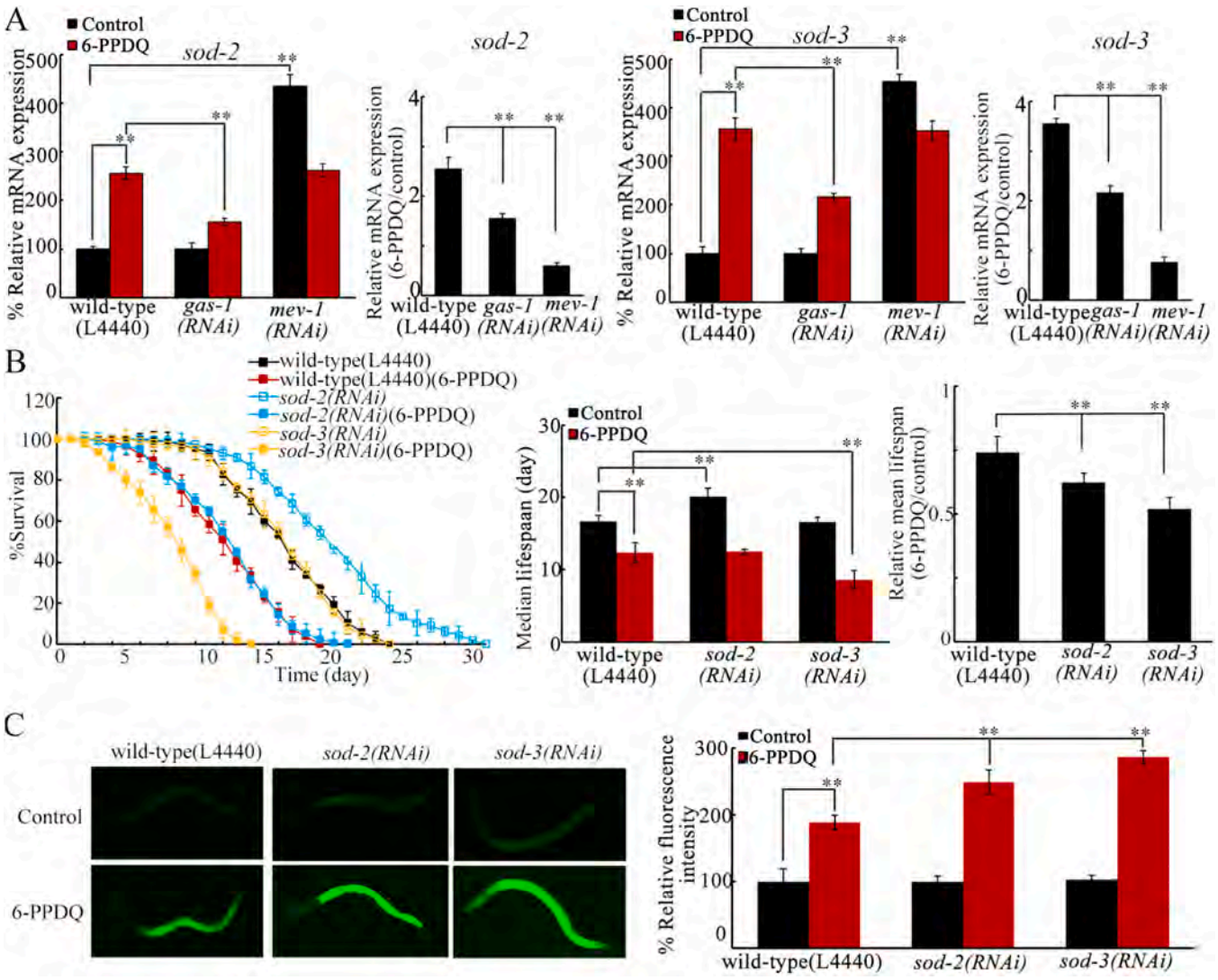

Fig. 7. Effect of RNAi of *gas-1* and *mev-1* on expressions of genes encoding mitochondrial Mn-SODs in 6-PPDQ exposed nematodes. (A) Effect of RNAi of *gas-1* or *mev-1* on expressions of *sod-2* and *sod-3* in 6-PPDQ exposed nematodes. (B) Effect of RNAi of *sod-2* or *sod-3* on lifespan in 6-PPDQ exposed nematodes. (C) Effect of RNAi of *sod-2* or *sod-3* on ROS production in 6-PPDQ exposed nematodes. Control, without 6-PPDQ exposure. Exposure concentration of 6-PPDQ was 10 μg/L. L4440, empty vector. Bars represent means ± SD. $^{**}P < 0.01$.

causes defects in mitochondrial complexes I and II and induces mitochondrial dysfunction. Emerging evidence reveals that mitochondrial complex defects can aggravate mitochondrial dysfunction and induce mitochondrial diseases, such as Parkinson's disease, Alzheimer's disease, and diabetes mellitus [63].

Mitochondrial dysfunction plays a crucial role in regulating longevity [64]. In *C. elegans*, there is increasing evidence that the mitochondrial complexes are associated with alteration of lifespan [53]. For example, the lifespan of *gas-1* mutant was lower than that of wild-type nematodes [65]. In addition, a shorter lifespan was also observed in *mev-1* mutant nematodes [66]. Following exposure, RNAi of *gas-1* and *mev-1* rendered nematodes vulnerable to 6-PPDQ toxicity in terms of reducing lifespan (Figs. 4A and 4C), demonstrating that the decrease in expressions of *gas-1* and *mev-1* mediated the effect of 6-PPDQ toxicity on lifespan. Additionally, double RNAi of *gas-1* and *mev-1* caused a more severe reduction in lifespan than in single RNAi of *gas-1* or *mev-1* in 6-PPDQ exposed nematodes (Fig. 4D), suggesting that GAS-1 and MEV-1 and their corresponding electron transfer chains functioned in parallel to regulate 6-PPDQ toxicity on lifespan. Nevertheless, in 6-PPDQ exposed nematodes, we found that RNAi of *nuo-1* did not affect lifespan (Fig. 4B). In complex I, the altered NUO-1 levels may be associated with other unknown effects (s) of 6-PPDQ on nematodes.

4.3. Disrupted mitochondrial complex I and II was associated with lifespan reduction in 6-PPDQ exposed nematodes

To determine how GAS-1 and MEV-1 regulate the effect of 6-PPDQ toxicity on lifespan, we identified insulin peptides as downstream targets in *C. elegans*. The insulin peptides INS-6, INS-7, and DAF-28 have been implicated in controlling the effects of 6-PPDQ toxicity on lifespan [32]. Following 6-PPDQ exposure, RNAi of *gas-1* and *mev-1* increased the expression of *ins-6*, *ins-7*, and *daf-28* (Figs. 5A and 5B). In addition, the susceptibility of *gas-1(RNAi)* and *mev-1(RNAi)* nematodes to 6-PPDQ toxicity in reducing lifespan was suppressed by RNAi targeting these three genes (Figs. 5C and 5D). Therefore, GAS-1 and MEV-1 jointly inhibited the expression and function of these three insulin peptides to regulate the 6-PPDQ toxicity on lifespan. In other words, GAS-1 and MEV-1 could act upstream of these three insulin peptides to control 6-PPDQ toxicity in reducing lifespan. Nevertheless, it remains unclear whether GAS-1 and MEV-1 can regulate 6-PPDQ toxicity by targeting specific targets.

In the insulin pathway, in addition to the insulin peptide genes, the

expression of the insulin receptor gene *daf-2* and its downstream kinase genes (*age-1*, *akt-1*, and *akt-2*) was also increased, and the FOXO transcriptional factor gene *daf-16* was decreased by RNAi of *gas-1* and *mev-1* in nematodes exposed to 6-PPDQ (Figs. 6A and 6B). In addition, the toxicity of 6-PPDQ on the lifespan of *gas-1(RNAi)* and *mev-1(RNAi)* nematodes was further reduced by RNAi of *daf-2* (Figs. 6C and 6D). The functions of DAF-2, AGE-1, AKT-1, AKT-2, and DAF-16 in regulating 6-PPDQ toxicity in reducing lifespan have been previously observed [32]. These observations further confirmed the role of the insulin signaling pathway as a downstream molecular event of GAS-1 and MEV-1 in regulating 6-PPDQ toxicity in nematodes.

In *C. elegans*, the alterations of mitochondrial complexes are associated with both longevity and oxidative stress [38]. Mutants of *gas-1* and *mev-1* are reported to be sensitive to oxidative stress [66,67]. The *sod-2* and *sod-3* encoding Mn-SODs were identified as downstream targeted genes of DAF-16 during the control of 6-PPDQ toxicity in reducing lifespan (Figs. S2 and 7B) [32]. Meanwhile, the relative expressions (6-PPDQ/control) of *sod-2* and *sod-3* were also observed in *gas-1(RNAi)* and *mev-1(RNAi)* nematodes exposed to 6-PPDQ (Fig. 7A). In addition, RNAi *sod-2* and *sod-3* increased the susceptibility of 6-PPDQ toxicity to induce ROS production (Fig. 7C). These results indicate that, under normal conditions, GAS-1 and MEV-1 can inhibit ROS scavenging by affecting the upstream insulin signaling pathway and activating Mn-SODs in the mitochondria. However, under 6-PPDQ exposure conditions, the decrease in GAS-1 and MEV-1 caused the inhibition of Mn-SODs and an increase in ROS production, which contributed to the reduction in lifespan.

5. Conclusions

Together, we observed the damage caused by 6-PPDQ at ERCs (1 and 10 μg/L) on mitochondrial functions reflected by altered oxygen consumption and ATP content in nematodes. These disrupted mitochondrial functions were associated with decreased activities of complexes I and II and decreased expression of *gas-1*, *nuo-1*, and *mev-1* encoding components of complexes I and II. Meanwhile, the decreased expression of *gas-1* and *mev-1* mediated 6-PPDQ toxicity in reducing lifespan. During the control of 6-PPDQ toxicity in reducing lifespan, GAS-1 and MEV-1 inhibited the expression of insulin peptides (INS-6, INS-7, and DAF-28) and insulin receptor DAF-2 and activated the FOXO transcriptional factor DAF-16 and its targets SOD-2 and SOD-3 to suppress the induction of oxidative stress. These results suggest the potential of 6-PPDQ in damaging mitochondrial functions and the activities of complexes I and II, which was associated with the induction of 6-PPDQ toxicity on lifespan by affecting the insulin signaling pathway in organisms. Nevertheless, in the current study, we only examined the effect of 6-PPDQ on complex I and II and their association with lifespan reduction. The effect of 6-PPDQ exposure at ERCs on other mitochondrial complexes and their association with induction of 6-PPDQ toxicity are suggested to be further determined.

Environmental implication

The 6-PPD quinone (6-PPDQ) has been widely distributed in the environment and showed bioavailability to environmental organisms. In *Caenorhabditis elegans*, 6-PPDQ at environmentally relevant concentrations (ERCs) could result in mitochondrial dysfunction, which was associated with altered activities and expressions of genes encoding components in complex I and II. Moreover, components on complex I and II regulated 6-PPDQ toxicity in reducing lifespan by inhibiting insulin peptides and receptor DAF-2. Our results suggested possibility of 6-PPDQ at ERCs in causing damage on mitochondrial complexes and in reducing lifespan in organisms.

CRediT authorship contribution statement

Jie Chao: Supervision. **Dayong Wang:** Writing – review & editing, Supervision. **Xin Hua:** Writing – original draft, Investigation. **Geyu Liang:** Supervision.

Declaration of Competing Interest

The authors declare that they have no known competing financial interests or personal relationships that could have appeared to influence the work reported in this paper.

Data Availability

The data that has been used is confidential.

Acknowledgment

This study was supported by the grant from Shenzhen Basic Research Project (JCYJ20220530163605011).

Appendix A. Supporting information

Supplementary data associated with this article can be found in the online version at doi:10.1016/j.jhazmat.2024.134598.

References

[1] Tian, Z., Zhao, H., Peter, K.T., Gonzalez, M., Wetzel, J., Wu, C., et al., 2021. A ubiquitous tire rubber-derived chemical induces acute mortality in coho salmon. Science 371, 185–189.
[2] Fohet, L., Andanson, J.M., Charbouillot, T., Malosse, L., Leremboure, M., Delor-Jestin, F., et al., 2023. Time-concentration profiles of tire particle additives and transformation products under natural and artificial aging. Sci Total Environ 859, 160150.
[3] Rauert, C., Charlton, N., Okoffo, E.D., Stanton, R.S., Agua, A.R., Pirrung, M.C., et al., 2022. Concentrations of the tire additive chemicals and tire road wear particles in an Australian urban tributary. Environ Sci Technol 56, 2421–2431.
[4] Chen, X., He, T., Yang, X., Gan, Y., Qing, X., Wang, J., et al., 2023. Analysis, environmental occurrence, fate and potential toxicity of tire wear compounds 6PPD and 6PPD-quinone. J Hazard Mater 452, 131245.
[5] Zhang, H., Huang, Z., Liu, Y., Hu, L., He, L., Liu, Y., et al., 2023. Occurrence and risks of 23 tire additives and their transformation products in an urban water system. Environ Int 171, 107715.
[6] Huang, W., Shi, Y., Huang, J., Deng, C., Tang, S., Liu, X., et al., 2021. Occurrence of substituted *p*-phenylenediamine antioxidants in dusts. Environ Sci Technol 8, 381–385.
[7] Hiki, K., Yamamoto, H., 2022. Concentration and leachability of *N*-(1,3-dimethylbutyl)-*N*′-phenyl-p-phenylenediamine (6-PPD) and its quinone transformation product (6PPD-Q) in road dust collected in Tokyo, Japan. Environ Pollut 302, 119082.
[8] Zeng, L., Li, Y., Sun, Y., Liu, L.Y., Shen, M., Du, B., 2023. Widespread occurrence and transport of p-phenylenediamines and their quinones in sediments across urban rivers, estuaries, coasts, and deep-sea regions. Environ Sci Technol 57, 2393–2403.
[9] Fang, L., Fang, C., Di, S., Yu, Y., Wang, C., Wang, X., et al., 2023. Oral exposure to tire rubber-derived contaminant 6PPD and 6PPD-quinone induce hepatotoxicity in mice. Sci Total Environ 869, 161836.
[10] Hua, X., Wang, D.-Y., 2023. Tire-rubber related pollutant 6-PPD quinone: a review of its transformation, environmental distribution, bioavailability, and toxicity. J Hazard Mater 459, 132265.
[11] Greer, J.B., Dalsky, E.M., Lane, R.F., Hansen, J.D., 2023. Tire-derived transformation product 6PPD-quinone induces mortality and transcriptionally disrupts vascular permeability pathways in developing coho salmon. Environ Sci Technol 57, 10940–10950.
[12] Ricarte, M., Prats, E., Montemurro, N., Bedrossiantz, J., Bellot, M., Gómez-Canela, C., et al., 2023. Environmental concentrations of tire rubber-derived 6PPD-quinone alter CNS function in zebrafish larvae. Sci Total Environ 896, 165240.
[13] Zhang, S.Y., Gan, X., Shen, B., Jiang, J., Shen, H., Lei, Y., et al., 2023. 6PPD and its metabolite 6PPDQ induce different developmental toxicities and phenotypes in embryonic zebrafish. J Hazard Mater 455, 131601.
[14] He, W.-M., Gu, A.-H., Wang, D.-Y., 2023. Four-week repeated exposure to tire-derived 6-PPD quinone causes multiple organ injury in male BALB/c mice. Sci Total Environ 894, 164842.
[15] Zhao, H.N., Thomas, S.P., Zylka, M.J., Dorrestein, P.C., Hu, W., 2023. Urine excretion, organ distribution, and placental transfer of 6PPD and 6PPD-quinone in

mice and potential developmental toxicity through nuclear receptor pathways. Environ Sci Technol 57, 13429–13438.
[16] He, W.-M., Chao, J., Gu, A.-H., Wang, D.-Y., 2024. Evaluation of 6-PPD quinone toxicity on lung of male BALB/c mice by quantitative proteomics. Sci Total Environ 922, 171220.
[17] Wang, D.-Y., 2020. Exposure Toxicology in *Caenorhabditis elegans*. Springer Nature Singapore Pte Ltd.
[18] Shao, Y., Hua, X., Li, Y., Wang, D., 2024. Comparison of reproductive toxicity between pristine and aged polylactic acid microplastics in *Caenorhabditis elegans*. J Hazard Mater 466, 133545.
[19] Wang, Y., Yuan, X., Zhou, R., Bu, Y., Wang, D., 2023. Combinational exposure to hydroxyatrazine increases neurotoxicity of polystyrene nanoparticles on *Caenorhabditis elegans*. Sci Total Environ 880, 163283.
[20] Wang, D.-Y., 2022. Toxicology at Environmentally Relevant Concentrations in *Caenorhabditis elegans*. Springer Nature Singapore Pte Ltd.
[21] He, W., Gu, A., Wang, D., 2023. Sulfonate-modified polystyrene nanoparticle at precited environmental concentrations induces transgenerational toxicity associated with increase in germline Notch signal of *Caenorhabditis elegans*. Toxics 11, 511.
[22] Hua, X., Cao, C., Zhang, L., Wang, D., 2023. Activation of FGF signal in germline mediates transgenerational toxicity of polystyrene nanoparticles at predicted environmental concentrations in *Caenorhabditis elegans*. J Hazard Mater 2023 (451), 131174.
[23] Liu, Z., Hua, X., Zhao, Y., Bian, Q., Wang, D., 2024. Polyethylene nanoplastics cause reproductive toxicity associated with activation of both estrogenic hormone receptor NHR-14 and DNA damage checkpoints in *C. elegans*. Sci Total Environ 906, 167471.
[24] Hua, X., Feng, X., Liang, G.-Y., Chao, J., Wang, D.-Y., 2023. Long-term exposure to tire-derived 6-PPD quinone causes intestinal toxicity by affecting functional state of intestinal barrier in *Caenorhabditis elegans*. Sci Total Environ 861, 160591.
[25] Hua, X., Feng, X., Liang, G.-Y., Chao, J., Wang, D.-Y., 2023. Exposure to 6-PPD quinone at environmentally relevant concentrations causes abnormal locomotion behaviors and neurodegeneration in *Caenorhabditis elegans*. Environ Sci Technol 57, 4940–4950.
[26] Hua, X., Feng, X., Liang, G.-Y., Chao, J., Wang, D.-Y., 2023. Long-term exposure to 6-PPD quinone reduces reproductive capacity by enhancing germline apoptosis associated with activation of both DNA damage and cell corpse engulfment in *Caenorhabditis elegans*. J Hazard Mater 454, 131495.
[27] Liu, Z.-Y., Bian, Q., Wang, D.-Y., 2024. Exposure to 6-PPD quinone causes ferroptosis activation associated with induction of reproductive toxicity in *Caenorhabditis elegans*. J Hazard Mater 471, 134356.
[28] Hua, X., Wang, D.-Y., 2024. Polyethylene nanoparticles at environmentally relevant concentrations enhances neurotoxicity and accumulation of 6-PPD quinone in *Caenorhabditis elegans*. Sci Total Environ 918, 170760.
[29] Wang, Y.-X., Liang, G.-Y., Chao, J., Wang, D.-Y., 2024. Comparison of intestinal toxicity in enhancing intestinal permeability and in causing ROS production of six PPD quinones in *Caenorhabditis elegans*. Sci Total Environ 927, 172306.
[30] Hua, X., Wang, D.-Y., 2023. Disruption of dopamine metabolism by exposure to 6-PPD quinone in *Caenorhabditis elegans*. Environ Pollut 337, 122649.
[31] Wang, Y.-X., Hua, X., Wang, D.-Y., 2023. Exposure to 6-PPD quinone enhances lipid accumulation through activating metabolic sensors of SBP-1 and MDT-15 in *Caenorhabditis elegans*. Environ Pollut 333, 121937.
[32] Hua, X., Wang, D.-Y., 2023. Exposure to 6-PPD quinone at environmentally relevant concentrations inhibits both lifespan and healthspan in *C. elegans*. Environ Sci Technol 57, 19295–19303.
[33] Ma, K., Chen, G., Li, W., Kepp, O., Zhu, Y., Chen, Q., 2020. Mitophagy, mitochondrial homeostasis, and cell fate. Front Cell Dev Biol 8, 467.
[34] Meyer, J.N., Hartman, J.H., Mello, D.F., 2018. Mitochondrial toxicity. Toxicol Sci 162, 15–23.
[35] Varshney, S., Gora, A.H., Siriyappagouder, P., Kiron, V., Olsvik, P.A., 2022. Toxicological effects of 6PPD and 6PPD quinine in zebrafish larvae. J Hazard Mater 424, 127623.
[36] Mahoney, H., da, Silver, Junior, F.C., Roberts, C., Schultz, M., Ji, X., et al., 2022. Exposure to the tire rubber-derived contaminant 6PPD-quinon causes mitochondrial dysfunction in vitro. Environ Sci Technol Lett 9, 765–771.
[37] Martins, A.C., Virgolini, M.B., Ávila, D.S., Scharf, P., Li, J., Tinkov, A.A., et al., 2023. Mitochondria in the spotlight: *C. elegans* as a model organism to evaluate xenobiotic-induced dysfunction. Cells 12, 2124.
[38] Sedensky, M.M., Morgan, P.G., 2006. Mitochondrial respiration and reactive oxygen species in *C. elegans*. Exp Gerontol 41, 957–967.
[39] Ishii, T., Miyazawa, M., Onouchi, H., Yasuda, K., Hartman, P.S., Ishii, N., 2013. Model animals for the study of oxidative stress from complex II. Biochim Biophys Acta 1827, 588–597.
[40] Wang, D.-Y., 2019. Molecular Toxicology in *Caenorhabditis elegans*. Springer Nature Singapore Pte Ltd.
[41] Brenner, S., 1974. The genetics of *Caenorhabditis elegans*. Genetics 77, 71–94.
[42] Zhuang, Z., Liu, T., Liu, Z., Wang, D., 2024. Polystyrene nanoparticles strengthen high glucose toxicity associated with alteration in insulin signaling pathway in *C. elegans*. Ecotoxicol Environ Saf 272, 116056.
[43] Tang, M., Ding, G., Li, L., Xiao, G., Wang, D., 2023. Exposure to polystyrene nanoparticles at predicted environmental concentrations enhances toxic effects of *Acinetobacter johnsonii* AC15 infection on *Caenorhabditis elegans*. Ecotoxicol Environ Saf 262, 115131.
[44] Elefantova, K., Lakatos, B., Kubickova, J., Sulova, Z., Breier, A., 2018. Detection of the mitochondrial membrane potential by the cationic dye JC-1 in L1210 cells with massive overexpression of the plasma membrane ABCB1 drug transporter. Int J Mol Sci 19, 1985.
[45] Will, Y., Hynes, J., Ogurtsov, V.I., Papkovsky, D.B., 2006. Analysis of mitochondrial function using phosphorescent oxygen-sensitive probes. Nat Protoc 1, 2563–2572.
[46] Zhang, X., Zuo, X., Yang, B., Li, Z., Xue, Y., Zhou, Y., et al., 2014. MicroRNA directly enhances mitochondrial translation during muscle differentiation. Cell 158, 607–619.
[47] Vercellino, I., Sazanov, L.A., 2022. The assembly, regulation and function of the mitochondrial respiratory chain. Nat Rev Mol Cell Biol 23, 141–161.
[48] Xu, C., Hwang, W., Jeong, D.E., Ryu, Y., Ha, C.M., Lee, S.V., et al., 2018. Genetic inhibition of an ATP synthase subunit extends lifespan in *C. elegans*. Sci Rep 8, 4836.
[49] Liu, T., Zhuang, Z., Wang, D., 2023. Paeoniflorin mitigates high glucose-induced lifespan reduction by inhibiting insulin signaling in *Caenorhabditis elegans*. Front Pharmacol 14, 1202379.
[50] Zhang, L., Wang, Y.-X., Wang, D.-Y., 2023. Paeoniflorin increases the survival of *Pseudomonas aeruginosa* infected *Caenorhabditis elegans* at the immunosuppression stage by activating PMK-1, BAR-1, and EGL-1 signals. Arch Pharm Res 46, 616–628.
[51] Shao, Y.-T., Wang, Y.-X., Hua, X., Li, Y.-H., Wang, D.-Y., 2023. Polylactic acid microparticles in the range of μg/L reduce reproductive capacity by affecting the gonad development and the germline apoptosis in *Caenorhabditis elegans*. Chemosphere 336, 139193.
[52] Wang, Y.-X., Zhang, L., Yuan, X.-A., Wang, D.-Y., 2023. Treatment with paeoniflorin increases lifespan of *Pseudomonas aeruginosa* infected *Caenorhabditis elegans* by inhibiting bacterial accumulation in intestinal lumen and biofilm formation. Front Pharmacol 14, 1114219.
[53] Chen, P.X., Zhang, L., Chen, D., Tian, Y., 2024. Mitochondrial stress and aging: Lessons from *C. elegans*. Semin Cell Dev Biol 154 69–76.
[54] Suthammarak, W., Somerlot, B.H., Opheim, E., Sedensky, M., Morgan, P.G., 2013. Novel interactions between mitochondrial superoxide dismutases and the electron transport chain. Aging Cell 12, 1132–1140.
[55] Fang, J., Wang, X., Cao, G., Wang, F., Ru, Y., Wang, B., et al., 2024. 6PPD-quinone exposure induces neuronal mitochondrial dysfunction to exacerbate Lewy neurites formation induced by α-synuclein preformed fibrils seeding. J Hazard Mater 465, 133312.
[56] Brinkmann, M., Montgomery, D., Selinger, S., Miller, J.G.P., Stock, E., Alcaraz, A. J., et al., 2022. Acute toxicity of the tire rubber-derived chemical 6PPD-quinne to four fishes of commercial, cultural, and ecological importance. Environ Sci Technol Lett 9, 333–338.
[57] Prosser, R.S., Salole, J., Hang, S., 2023. Toxicity of 6PPD-quinone to four freshwater invertebrate species. Environ Pollut 337, 122512.
[58] Challis, J.K., Popick, H., Prajapati, S., Harder, P., Giesy, J.P., McPhedran, K., et al., 2021. Occurrences of tire rubber-derived contaminants in cold-climate urban runoff. Environ Sci Technol Lett 8, 961–967.
[59] Seiwert, B., Nihemaiti, M., Troussier, M., Weyrauch, S., Reemtsma, T., 2022. Abiotic oxidative transformation of 6-PPD and 6-PPD quinone from tires and occurrence of their products in snow from urban roads and in municipal wastewater. Water Res 212, 118122.
[60] Berry, B.J., Vodičková, A., Müller-Eigner, A., Meng, C., Ludwig, C., Kaeberlein, M., et al., 2023. Optogenetic rejuvenation of mitochondrial membrane potential extends *C. elegans* lifespan. Nat Aging 3, 157–161.
[61] van der Bliek, A.M., Sedensky, M.M., Morgan, P.G., 2017. Cell biology of the mitochondrion. Genetics 207, 843–871.
[62] Rich, P.R., Maréchal, A., 2010. The mitochondrial respiratory chain. Essays Biochem 47, 1–23.
[63] Schapira, A.H., 2012. Mitochondrial diseases. Lancet 379, 1825–1834.
[64] Guo, Y., Guan, T., Shafiq, K., Yu, Q., Jiao, X., Na, D., et al., 2023. Mitochondrial dysfunction in aging. Ageing Res Rev 88, 101955.
[65] McCormack, S., Polyak, E., Ostrovsky, J., Dingley, S.D., Rao, M., Kwon, Y.J., et al., 2015. Pharmacologic targeting of sirtuin and PPAR signaling improves longevity and mitochondrial physiology in respiratory chain complex I mutant *Caenorhabditis elegans*. Mitochondrion 22, 45–59.
[66] Kayser, E.B., Sedensky, M.M., Morgan, P.G., 2004. The effects of complex I function and oxidative damage on lifespan and anesthetic sensitivity in *Caenorhabditis elegans*. Mech Ageing Dev 125 455–464.
[67] Brand, M.D., 2000. Uncoupling to survive? The role of mitochondrial inefficiency in ageing. Exp Gerontol 35, 811–820.